Marquette University
e-Publications@Marquette

Physics Faculty Research and Publications | Physics, Department of

The Metallo-β-lactamase GOB Is a Mono-Zn(II) Enzyme with a Novel Active Site

Jorgelina Morrán-Barrio
Universidad Nacional de Rosario

Javier M. Gonzalez
Universidad Nacional de Rosario

Mariá Natalia Lisa
Universidad Nacional de Rosario

Alison L. Costello
University of New Mexico

Matteo Dal Peraro
University of Pennsylvania

See next page for additional authors

Authors

Jorgelina Morrán-Barrio, Javier M. Gonzalez, Mariá Natalia Lisa, Alison L. Costello, Matteo Dal Peraro, Paolo Carloni, Brian Bennett, David L. Tierney, Adriana S. Limansky, Alejandro M. Viale, and Alejandro J. Vila

The Metallo-β-lactamase GOB Is a Mono-Zn(II) Enzyme with a Novel Active Site*[S]

Jorgelina Morán-Barrio[‡1,2], **Javier M. González**[‡1,3], **María Natalia Lisa**[‡], **Alison L. Costello**[§], **Matteo Dal Peraro**[¶],
Paolo Carloni[‖4], **Brian Bennett**[**5], **David L. Tierney**[§], **Adriana S. Limansky**[‡6], **Alejandro M. Viale**[‡7],
and Alejandro J. Vila[‡8]

From the ‡Departamento de Química Biológica and Departamento de Microbiología, Instituto de Biología Molecular y Celular de
Rosario (IBR), Facultad de Ciencias Bioquímicas y Farmacéuticas, Universidad Nacional de Rosario, Suipacha 531, S2002LRK
Rosario, Argentina, the §Department of Chemistry, University of New Mexico, Albuquerque, New Mexico 87131, the ¶Center for
Molecular Modeling, University of Pennsylvania, Philadelphia, Pennsylvania 19104, the ‖International School for Advanced Studies,
Via Beirut 2-4, 34100 Trieste, Italy, and the **National Biomedical EPR Center, Department of Biophysics, Medical College of
Wisconsin, Milwaukee, Wisconsin 53226-0509

Metallo-β-lactamases (MβLs) are zinc-dependent enzymes
able to hydrolyze and inactivate most β-lactam antibiotics. The
large diversity of active site structures and metal content among
MβLs from different sources has limited the design of a pan-
MβL inhibitor. Here we report the biochemical and biophysical
characterization of a novel MβL, GOB-18, from a clinical isolate
of a Gram-negative opportunistic pathogen, *Elizabethkingia
meningoseptica*. Different spectroscopic techniques, three-di-
mensional modeling, and mutagenesis experiments, reveal that
the Zn(II) ion is bound to Asp^{120}, His^{121}, His^{263}, and a solvent
molecule, *i.e.* in the canonical Zn2 site of dinuclear MβLs. Con-
trasting all other related MβLs, GOB-18 is fully active against a
broad range of β-lactam substrates using a single Zn(II) ion in
this site. These data further enlarge the structural diversity of
MβLs.

The expression of β-lactam degrading enzymes (β-lactama-
ses) is the most common mechanism of antibiotic resistance
among bacteria (1, 2). These enzymes have been grouped into
four classes (A–D) according to sequence homology (3, 4).
Class A, C, and D enzymes use an active site serine residue as a
nucleophile, whereas class B lactamases (generically termed
metallo-β-lactamases, MβLs)[9] employ one or two Zn(II) ions to
cleave the β-lactam ring.

MβLs have particular importance in the clinical setting since
they can hydrolyze a broader spectrum of β-lactam substrates
than the serine-type enzymes and are resistant to most clini-
cally employed inhibitors (5–11). The design of an efficient
pan-MβL inhibitor has been mostly limited by a striking diver-
sity in the active site structures, catalytic features, and metal ion
requirements for activity among different enzymes. Based on
this heterogeneity, MβLs have been classified into three sub-
classes: B1, B2, and B3 (3, 6). Subclass B1 includes several chro-
mosomally encoded enzymes such as BcII from *Bacillus cereus*
(12–14), CcrA from *Bacteroides fragilis* (15–18), BlaB from
Elizabethkingia meningoseptica (formerly, *Chryseobacterium
meningosepticum*) (19), as well as the transferable VIM (20)-,
IMP (21, 22)-, SPM (23, 24)-, and GIM-type enzymes. Subclass
B2 includes the CphA (25, 26) and ImiS (27) lactamases from
Aeromonas species. Subclass B3, originally represented only by
L1 from *Stenotrophomonas maltophilia* (28–30), now includes
enzymes from other opportunistic pathogens like FEZ-1 from
Legionella gormanii (31) and GOB from *E. meningoseptica* (32),
as well as from environmental bacteria such as CAU-1 from
Caulobacter crescentus (33) and THIN-B from *Janthinobacte-
rium lividum* (34).

Molecular structures of MβLs from the three subclasses have
been solved by x-ray crystallography (12, 14, 15, 25, 31). Com-
parison of the tertiary structure of enzymes belonging to the
different subclasses reveals a common $\alpha\beta/\beta\alpha$ sandwich fold, in
which different insertions and deletions have resulted in differ-
ent loop topologies and, ultimately, in different zinc coordina-
tion environments and metal site occupancies among B1, B2,
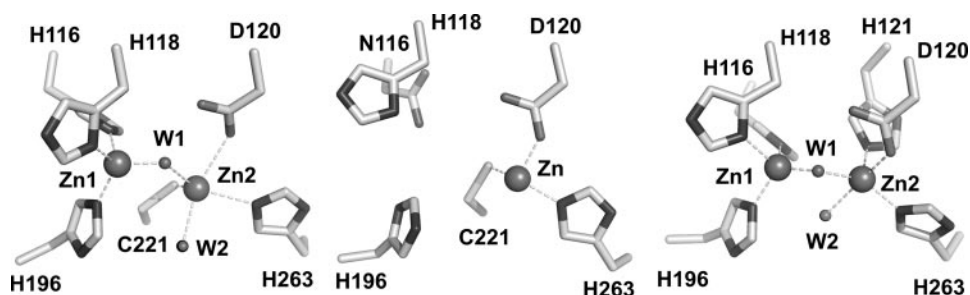and B3 enzymes (Fig. 1). MβLs bind up to two metal ions in

FIGURE 1. **Metallo-β-lactamase metal binding sites:** *B. cereus* BcII (B1, Protein Data Bank code 1bc2, *left*) **(14),** *A. hydrophila* CphA (B2, Protein Data Bank code 1x8g, *center*) **(25), and** *S. maltophilia* L1 (B3, Protein Data Bank code 1sml, *right*) **(28).** Zinc atoms are shown as *gray spheres*, and water molecules (*W*) are shown as *small gray spheres*. Coordination bonds are shown as *dashed lines*.

their active sites. In B1 and B3 enzymes, one Zn(II) ion (Zn1) is tetrahedrally coordinated to three histidine ligands (His[116], His[118], and His[196] in Fig. 1) and a water/OH$^-$ molecule (3-H site) (14, 15, 28). The coordination polyhedron of Zn2 in B1 enzymes is provided by Asp[120], Cys[221], His[263], and one or two-water molecules (DCH site). Notably, this site represents the active species in mono-Zn(II) B2 enzymes (25). Instead, two mutations (Cys[221] → Ser and Arg[121] → His) affect the Zn2 coordination geometry in B3 MβLs, and the metal ion is bound to Asp[120], His[121], His[263], and one- or two-water molecules, while Ser[221] is no longer a metal ligand (DHH site) (28). A remarkable exception is provided by the deepest branching member of the MβL B3 subclass, GOB from *E. meningoseptica* (4). In all reported GOB sequences, His[116] and Ser[221] are substituted by Gln and Met, respectively, suggesting the presence of an unusually perturbed metal binding site.

Here we show that *E. meningoseptica* GOB-18 represents a novel type of broad spectrum MβL unique in being maximally active in the mono-Zn(II) form and in which the metal ion occupies only the Zn2, DHH site. This contrasts with two generally accepted ideas: broad spectrum MβLs are maximally active in the dinuclear form (B1 and B3 enzymes), and mono-Zn(II) enzymes are carbapenemases (B2 enzymes). Finally, the findings presented here confirm that Zn2 is central for MβL-mediated catalysis and that the attacking nucleophile could be provided either by a non-metal center or by the Zn2 site. This claims for a revisited strategy for the design of broad spectrum MβL inhibitors.

EXPERIMENTAL PROCEDURES

Source of GOB-18 Coding Sequence—An *E. meningoseptica* clinical strain from the Hospital Clemente Alvarez (Rosario, Argentina), identified by API 20NE (bioMerieux, Marcy l'Etoile, France), was used as the source of the genomic DNA for cloning the GOB-18 coding gene.

DNA Cloning and Construction of the Expression Vector for GOB-18—Genomic DNA from the *E. meningoseptica* clinical strain used here was isolated essentially as described in ref (35). The complete coding sequence of the *gob-18* gene was amplified by employing primers 1 and 2 described in Ref. 32. The DNA fragment was sequenced and two new primers were designed (see supplemental material) to clone the mature GOB-18 coding sequence cloned into BamHI-Hin-

dIII sites of pETGEXTerm vector (13) in frame to the 3′-end of *Schistosoma japonicus* glutathione *S*-transferase gene, for expression purposes. The resulting recombinant pET-GOB-18 plasmid produces GOB-18 as a C-terminal fusion to glutathione *S*-transferase. The nucleotide sequence reported in this paper was assigned accession number DQ004496 in the combined EMBL/GenBank^{TM}/DDBJ sequence data base.

Site-directed Mutagenesis—Site-directed mutagenesis was achieved using a rapid PCR-based method with modifications (36 and see supplemental material).

Protein Expression and Purification—GOB-18 wild-type and mutants were overproduced in *Escherichia coli* BL21(DE3) pLysS and *E. coli* BL21(DE3) Codon Plus RIL cells, respectively, transformed with plasmid pET-GOB-18, pET9a-Gln[116] → His GOB-18, pET9a-Asp[120] → Ser GOB-18, or pET9a-Cys[201] → Ser GOB-18. We followed protein expression and purification procedures described before (13) with modifications. The purification average yields were of ~12 mg of GOB-18 or Cys[201] → Ser GOB-18, 6 mg of Gln[116] → His GOB-18, and 3 mg of Asp[120] → Ser GOB-18, per liter of culture, and rendered polypeptides of 31 kDa at a purity higher than 95%, as estimated by SDS-PAGE (37). Pure enzymes were dialyzed twice against 100 volumes of 15 mM Hepes, pH 7.5, NaCl 0.2 M, pooled, and then stored at 4 °C for immediate use. The concentration of purified enzymes was determined by measuring the absorbance at 280 nm in a Jasco V-550 spectrophotometer, using the theoretically calculated molar extinction coefficient (32,200 M^{-1} cm^{-1} for GOB-18, Gln[116] → His GOB-18 or Asp[120] → Ser GOB-18, and 32,075 M^{-1} cm^{-1} for Cys[201] → Ser GOB-18) (38).

Biochemical Characterization of Wild-type GOB-18 and Mutants—Size exclusion chromatography was done on a Superdex 200 HR 10/30 column (Amersham Biosciences). The molecular mass of purified GOB-18 was measured by mass spectrometry/electrospray using an LCQ Duo Ion Trap mass spectrometer at the mass spectrometry facility LANAIS-PRO, University of Buenos Aires.

Circular Dichroism spectra of protein samples in 10 mM Tris-HCl, pH 7.5, and 50 mM NaCl were measured at 25 °C, using a Jasco J-715 spectropolarimeter flushed with N₂.

The amount of solvent exposed cysteine thiols in GOB-18 was determined employing 5,5′-dithiobis-(2-nitrobenzoic acid) in native and SDS-unfolded samples (39).

The GOB-18 and Gln[116] → His GOB-18 apoproteins were prepared by treating samples ~0.1 mM in 10 mM Tris-HCl, pH 7.0, with chelating agents in mild denaturing conditions (see supplemental material). The Zn(II) derivatives were prepared by dialyzing the apo-GOB-18 or apo-Gln[116] → His GOB-18 against 100 volumes of 10 mM Tris-HCl, pH 7.0, 50 mM NaCl, with an equimolar concentration of ZnSO₄. The Fe(II)-GOB-18 derivative was prepared in the same way using instead (NH₄)Fe(SO₄), under anaerobic conditions, with O₂-free N₂

efflux and addition of 1 mM sodium dithionite. The reduced state of the metal ion was verified colorimetrically using *o*-phenanthroline. The Fe(III)-GOB-18 derivative was prepared taking advantage of Zn(II) dissociation at acidic pH values retaining the iron content. Holo-GOB-18 was dialyzed against 100 volumes of polybuffer TAMS (50 mM Tris, 50 mM sodium acetate, 50 mM MES, and 500 mM NaCl) adjusted to pH 4.5 (twice). Then pH was raised by dialysis against 100 volumes of 10 mM Tris-HCl, pH 7, and 50 mM NaCl (twice).

Metal Content Determination—The metal content of the purified enzymes was measured by inductively coupled plasma-atomic emission spectrometer or by atomic absorption spectroscopy in a Metrolab 250 instrument operating in the flame mode.

Determination of IC$_{50}$ Value—The concentration required to effect 50% inhibition of enzyme activity (IC$_{50}$) was determined by preincubating GOB-18 (2 nM) in 15 mM Hepes, pH 7.5, 200 mM NaCl, 30 °C, with increasing EDTA concentrations for 1 min, prior to the initiation of the assay by the addition of 1 mM cefotaxime. A plot of steady-state hydrolysis rate *versus* inhibitor concentration provided the basis for the assessment of the IC$_{50}$ value.

Determination of the Kinetic Parameters—The hydrolysis of the antibiotics was monitored by following the absorbance variation resulting from the hydrolysis of the β-lactam ring. The reaction medium employed was 15 mM Hepes, pH 7.5, 0.2 M NaCl. All measurements were performed at 30 °C. The kinetic parameters K_m and k_{cat} were derived from initial rate measurements, recorded on a Jasco V-550 spectrophotometer, and were estimated by nonlinear data fitting to the integrated form of the Michaelis-Menten equation.

pH Dependence—The pH dependence of GOB-18-mediated cefotaxime hydrolysis was determined by performing measurements in the polybuffer TAMS adjusted from pH 4.0 to pH 8.0 with increments of 0.5 pH units, at 1 mM substrate concentration (see supplemental material).

X-ray Absorption Spectroscopy—Samples of GOB-18 (~1 mM) were prepared with 20% (v/v) glycerol, and loaded in Lucite cuvettes with 6-μm polypropylene windows, before rapid freezing in liquid nitrogen. X-ray absorption spectra were measured at the National Synchrotron Light Source (Brookhaven National Laboratory, Upton, NY), beamline X9B, with a Si(111) double crystal monochromator; harmonic rejection was accomplished using a nickel focusing mirror. Data collection and reduction were accomplished according to published procedures (40). XAS data were collected on two independently isolated samples. As each data set gave similar results, the spectra were averaged; the data in Fig. 3 represent the average of the two data sets (12 scans total).

Fourier filtered EXAFS data ($\Delta k = 1$–13 Å^{-1}; $\Delta r = 0.5$–2.1 Å, first shell or 0.1–4.5 Å for multiple scattering fits) were fit utilizing theoretical amplitude and phase functions calculated with FEFF v.8.00 (41). The zinc-nitrogen scale factor and the threshold energy, ΔE_0, were calibrated to the experimental spectrum for tetrakis-1-methylimidazole zinc(II) perchlorate, Zn(MeIm)$_4$ (42), and held fixed (at 0.78 and -21 eV, respectively), as were similarly determined values for iron (0.78 and -21 eV), in all subsequent fits to the data for GOB-18. First

shell fits were then obtained for all reasonable coordination numbers, including mixed nitrogen/oxygen ligation, while allowing the absorber-scatterer distance, R_{as}, and the Debye-Waller factor, σ_{as}^2, to vary; the best fits are presented in the supporting information. Multiple scattering contributions from histidine ligands were fit according to published procedures. Metal-metal (zinc-iron and iron-zinc) scattering was modeled with reference to the experimental EXAFS of Zn$_2$(salpn)$_2$ and Fe$_2$(salpn)$_2$.

NMR—NMR spectra were recorded on a Bruker Avance II 600 spectrometer operating at 600.13 MHz at different temperatures, as indicated. ^{1}H NMR spectra were recorded under conditions to optimize detection of the fast relaxing paramagnetic resonances, either using the superWEFT pulse sequence or water presaturation. Spectra were acquired over large spectral widths with acquisition times ranging from 16 to 80 ms and intermediate delays from 2 to 35 ms. One-dimensional experiments with solvent presaturation were used to record isotropically shifted signals closer to the diamagnetic envelope.

EPR—EPR was recorded at 9.63 GHz with 2-milliwatt microwave power and 5-G (0.5 mT) magnetic field modulation at 100 kHz, using a Bruker EleXsys E500 spectrometer equipped with an ER4116DM cavity operating in perpendicular mode and an Oxford Instruments ESR900 helium flow cryostat and ITC503 temperature controller.

RESULTS

Biochemical Characterization of GOB-18—The gene coding for a GOB-type MβL was cloned from a carbapenem-resistant *E. meningoseptica* clinical strain. Sequence analysis indicated a predicted molecular mass of 31.4 kDa for the encoded protein. At the time of sequencing there were 17 known variants of GOB enzymes. This protein differed from those reported previously and was named GOB-18. This enzyme differed from the firstly reported GOB enzyme, GOB-1 (32), by three conserved mutations: Leu^{94} → Phe, Ala^{137} → Val, and Asp^{282} → Asn (standard consensus numbering) (5).

Recombinant GOB-18 was overproduced as a fusion to GST in the cytoplasm of *E. coli* BL21(DE3) pLysS cells, cleaved, and purified to homogeneity. GOB-18 is a monomeric enzyme according to size exclusion chromatography. Mass spectrometry confirmed the molecular mass expected from the gene sequence. The β-lactamase activity (measured as cefotaxime hydrolysis) was inhibited by EDTA with an IC$_{50}$ of 2.3 ± 0.3 mM, indicating that GOB-18 holds a tightly bound divalent cation essential for activity. Inductively coupled plasma and atomic absorption analyses showed that recombinant GOB-18 contained significant amounts of zinc and, notably, iron. Although the relative amounts of these two metals varied among different enzyme preparations (0.45–0.75 iron/GOB-18 and 0.01–0.20 zinc/GOB-18), the total metal content never exceeded one metal ion per protein molecule. Addition of excess Zn(II) did not alter the CD spectrum of GOB-18 as isolated, neither in the near nor in the far UV (data not shown). Overall, these data suggest that GOB-18 is a mono-metallic enzyme, in sharp contrast to the other B3 MβLs.

The apoprotein was devoid of lactamase activity that could be recovered by addition of Zn(II). Remarkably, apo-GOB-18

remetallated with Zn(II) bound only one equivalent of Zn(II) and its activity largely exceeded that of the enzyme as isolated (Fig. 2). On the other hand, Fe(II)-GOB-18 and Fe(III)-GOB-18 displayed negligible activities compared with that of Zn(II)-GOB-18. In fact, Fe(III)-GOB-18 was poorly active even upon addition of Zn(II), suggesting that both metal ions compete for the same binding site. The kinetic parameters of Zn(II)-GOB-18, reported in Table 1, show that mono-Zn(II)-GOB-18 presents a broad substrate spectrum for β-lactams, similarly to that shown by dinuclear B3 enzymes. Addition of 20 μM Zn(II) to the reaction medium did not modify the enzyme kinetic parameters.

The pH dependence of GOB-18-mediated cefotaxime hydrolysis showed a plateau between pH values of 6 and 8, and an acidic limb, resulting in a complete inactivation at pH ≤ 4.5. This loss of activity could be reverted by raising the pH to 6.5, indicating that the inactivation is reversible. Metal content analysis at different pH values showed that the decrease in activity at low pH paralleled the dissociation of Zn(II) from the enzyme, despite the fact that most of the Fe(III) remained bound up to pH 4 (see supplemental material).

Overall, these data show that Zn(II)-GOB-18 is the active β-lactamase species. GOB-18 preparations with larger zinc/iron ratios were the most active ones, in line with this observation (see supplemental material). Expression of the complete GOB-18 gene (including a transit peptide sequence) in *E. coli* results in an enzyme secreted to the periplasm confering β-lac-

tam resistance to the bacterial host. Isoelectrofocusing analysis of the periplasmic fraction after osmotic shock revealed that the enzyme is present exclusively in the Zn(II) form, suggesting that iron uptake could be due to an artifact of protein overexpression in *E. coli* cytoplasm.

X-ray Absorption Spectroscopy—EXAFS data recorded at the zinc and iron edges, $k^3\chi((k)$, and the corresponding Fourier transforms for GOB-18 are shown in Fig. 3. EXAFS curve-fitting results are presented as supporting information. Fits to Fourier-filtered first shell scattering (0.5–2.1 Å) in the case of Zn(II)-GOB-18 suggest coordination to 4 nitrogen/oxygen donors at a distance of 2.01 Å (Fit Zn-1). Fit residuals did not improve significantly upon inclusion of a sulfur, or a mixed shell of nitrogen/oxygen. Multiple scattering analysis indicates ligation to 2 histidine residues (Fit Zn-2). The low Debye-Waller factor for the second multiple scattering path (C_1-N_1) most likely reflects some rotation of the imidazole plane about the axis normal to the zinc-nitrogen bond. Inclusion of a single zinc-carbon scattering interaction at a distance of 2.71 Å, representing carboxylate carbon scattering, modestly improved the fit (~15%) (Fit Zn-3).

In the case of Fe(III)-GOB-18, single shell fits give an average of 5 nitrogen/oxygen scatterers at 2.11 Å (Fit Fe-1). Inclusion of a sulfur atom increased the fit residual. The larger metal-ligand distance is consistent with a higher coordination number for iron relative to zinc. Separate shells of 3 oxygen atoms at 2.04 Å and 2 nitrogen atoms at 2.20 Å could be resolved (Fit Fe-2), and multiple scattering fits indicate the presence of two His ligands (Fit Fe-3). Inclusion of an iron scatterer in fits for Zn(II)-GOB-18 (Fit Zn-4) and a zinc scatterer in fits for Fe(III)-GOB-18 (Fit Fe-3) slightly improved the fits but led to different metal-metal distances (3.61 and 3.55 Å, respectively). This allows us to discard the existence of a heterodimetallic site in GOB-18. Thus, EXAFS data, together with the biochemical studies, suggest that Zn(II) and Fe(III) compete for the only metal binding site in GOB-18. Based on this, we decided to exploit Fe(III) as a spectroscopic probe of the metal site.

Spectroscopic Characterization of Fe(III)-GOB-18—The UV-visible spectrum of Fe(III)-GOB-18 revealed an absorption band centered at 375 nm, which was not present in the apoenzyme nor in the Zn(II)-reconstituted form (Fig. 4A). This feature can be attributed to a typical His-Fe(III) charge transfer band, similar to those observed in lipoxygenase, iron superoxide dismutase, and other non-heme, non-Fe-S iron proteins (43). EPR spectra of GOB-18 recorded at 6 K and 25 K (Fig. 4B) indicated an isolated, "rhombic" (*i.e.* mean $E/D \sim \frac{1}{3}$) Fe(III)

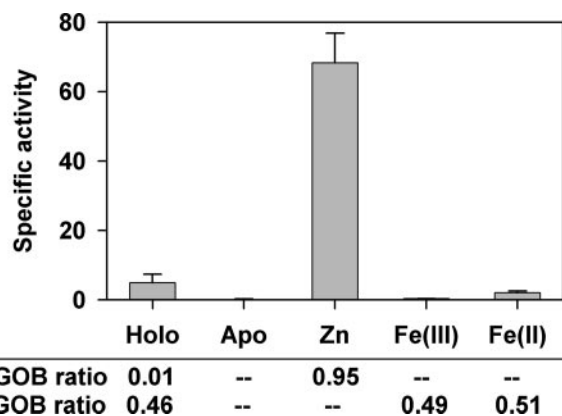|	Holo	Apo	Zn	Fe(III)	Fe(II)
Zn/GOB ratio	0.01	--	0.95	--	--
Fe/GOB ratio	0.46	--	--	0.49	0.51

FIGURE 2. **Activity of the different GOB-18 metal derivatives determined against 1 mM cefotaxime.** Specific activity was defined as the rate of hydrolysis (μM s^{-1}) per unit enzyme concentration (μM). Samples are: GOB-18 as isolated (*Holo*), apo-GOB-18 (*Apo*), Zn(II)-remetallated apo-GOB-18 (Zn(II)), Fe(III)-GOB-18 (Fe(III)), Fe(II)-GOB-18 (Fe(II)). GOB-18 metal derivatives were prepared as described under "Experimental Procedures." Metal content of each sample is detailed at the bottom. --, less than 0.001.

TABLE 1
Kinetic parameters for the hydrolysis of different β-lactam substrates by fully loaded wild type Zn(II)-GOB-18 and Zn(II)-Gln^{116} → His GOB-18 mutant

Kinetic parameters derived from a nonlinear fit of Michaelis-Menten equation to initial rate measurements. Reported values are the average of at least three independent enzyme preparations. ND, not determined.

	GOB-18			Gln^{116} → His GOB-18		
Substrate	k_{cat}	K_m	k_{cat}/K_m	k_{cat}	K_m	k_{cat}/K_m
	s^{-1}	μM	$\mu M^{-1} s^{-1}$	s^{-1}	μM	$\mu M^{-1} s^{-1}$
Penicillin G	680 ± 80	330 ± 30	2.1 ± 0.4	664 ± 9	380 ± 20	1.7 ± 0.1
Cefaloridine	30 ± 2	31.5 ± 0.5	0.95 ± 0.08	ND	ND	
Cefotaxime	83 ± 2	88 ± 6	0.94 ± 0.09	13.1 ± 0.1	58 ± 2	0.23 ± 0.01
Imipenem	42 ± 9	26 ± 2	1.6 ± 0.5	19.3 ± 0.4	58 ± 3	0.33 ± 0.02
Meropenem	72.5 ± 0.5	40 ± 10	1.8 ± 0.5	ND	ND	

ion. The almost complete loss of the $M_S = |\pm1/2\rangle$ (or $M_S = |\pm5/2\rangle$) signals at 25 K suggests a zero field splitting, Δ, of less than about 30 cm^{-1}. The asymmetry of the lines at $g_{\text{eff}} \sim 4.3$ and at $g_{\text{eff}} \sim 9$ indicates significant strain in E/D, although the shoulder on the crossover at $g_{\text{eff}} \sim 4.3$ (Fig. 4B, *inset*) indicates a lower degree of strain than in the often-seen "adventitious iron" signal and provides strong evidence for the Fe(III) being tightly protein-bound. In contrast to the iron-loaded glyoxylase II (44), no signals attributable to an Fe(III)-Fe(II) coupled system were observed from GOB-18.

^{1}H NMR spectra recorded under conditions that allow the detection of paramagnetic signals revealed a set of isotropically shifted resonances spanning from 100 to 20 ppm (Fig. 4C): a broad feature (A), accounting for three resonances centered at 80 ppm, a signal of fractional intensity at 38 ppm (B), and a two-proton resonance at 30 ppm (C). When the spectrum was recorded in D_2O, a loss of intensity corresponding to two protons was noticed in the broad envelope A, revealing the presence of two exchangeable resonances. The broad nature of these resonances is comparable with that reported for mononuclear Fe(III) enzymes such as protocatechuate dioxygenase (45), allowing us to discard the presence of a coupled, di-iron site. The two exchangeable resonances located at ~80 ppm can

be attributed to two His ligands, in agreement with the analysis of the EXAFS data. The broad nature of these signals prevented us to perform one-dimensional or two-dimensional nuclear Overhauser effect spectra to assign them.

Altogether, EPR, NMR, and EXAFS data allow us to rule out the formation of a dinuclear Fe(III) site in GOB-18, supporting the above assumption that Fe(III) and Zn(II) bind to the same site. EXAFS and NMR reveal the presence of two His ligands at the metal site, with five nitrogen/oxygen ligands for Fe(III). The ^{1}H NMR spectrum shows only 5–6 resonances corresponding to metal ligands, two of them corresponding to imidazolic His NHs, suggesting that one or two water molecules would be needed to achieve a penta-coordinated site.

This picture can be accounted for by two possibilities: (i) that the metal ion binds to a modified Site 1 in GOB-18, in which His116 has been replaced by a Gln residue, with His[118], His[196], and a H_2O/OH^- moiety completing the coordination sphere or (ii) by placing the metal ion into Site 2 (DHH ligand set), with Asp[120], His[121], His[263], and a H_2O/OH^- as metal ligands.

Three-dimensional Modeling—Three-dimensional models for Zn(II)-GOB-18 were built by homology modeling from the two available x-ray structures of B3 MβLs: FEZ-1 and L1 (38 and 21% sequence identity, respectively), including metal-ligand constraints based on spectroscopic data. We examined the possibility of binding a single Zn(II) ion to each of the two canonical metal binding sites. Best GOB-18 models for both mono-zinc active site conformations show low backbone root mean square deviation compared with FEZ-1 and L1 (0.6 and 1.5 Å, respectively), suggesting that the protein fold can accommodate a single Zn(II) ion in either binding site. Quantum chemical geometry optimizations based on density functional theory on unconstrained models of these metal sites with water or hydroxide as the fourth ligand suggested a regular tetrahedral geometry for a Zn(II) ion at a modified Site 1 and a distorted tetrahedron for the metal ion bound to Site 2. Predicted averaged zinc-nitrogen/oxygen distances are within ±0.04 Å from the values retrieved from EXAFS data, preventing us from discerning between the two sites (see supplemental material for additional "Experimental Procedures").

Site-directed Mutagenesis of Putative Metal Ligands—To unequivocally identify the metal binding site in GOB-18, we constructed mutants of possible metal ligands. In one of them
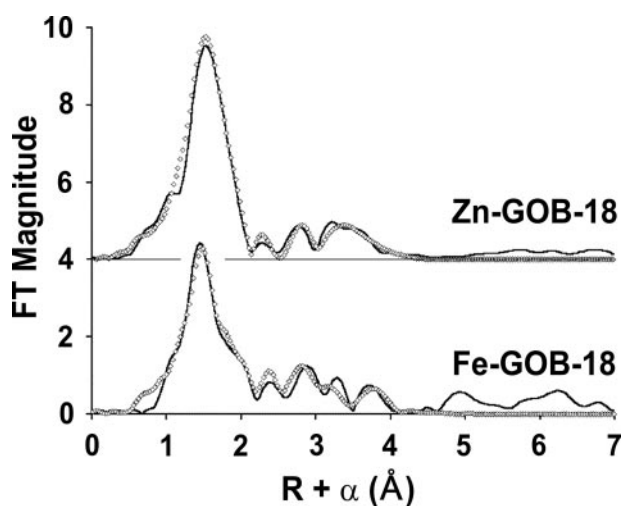

FIGURE 3. **Fourier transformed EXAFS data of mono-zinc (*top, solid lines*) and mono-iron (*bottom, solid lines*) GOB-18, and corresponding best fits (*open diamonds*).** The fits correspond to fits Zn-2 and Fe-3 in Table S1.
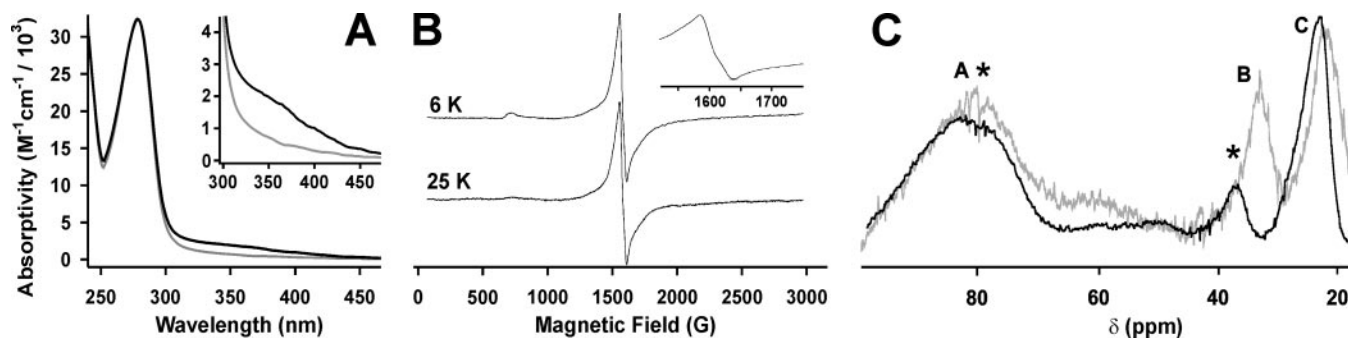

FIGURE 4. **Spectroscopic data on GOB-18.** *A*, UV-visible spectra of GOB-18 as isolated (*black line*) and apo-enzyme (*gray line*). The *inset* shows the His-Fe(III) charge transfer band at 375 nm. The corresponding spectrum of Zn(II)-GOB-18 is indistinguishable from that of apo-GOB-18 in the wavelength range shown. *B*, X-band EPR spectra of 300 μM GOB-18 in buffer 15 mM Hepes, pH 7.5, 0.2 M NaCl with 25% glycerol, at 6 K (*top*) and 25 K (*bottom*); the *inset* shows an expanded region of the spectrum recorded at 6 K. *C*, NMR spectra of GOB-18 and Gln[116] → His GOB-18 in buffer 15 mM Hepes, pH 7.5, 0.2 M NaCl with 10% D_2O. The enzymes were 1.1 mM. The intensity of signals indicated with * decrease in D_2O. *Black line*, GOB-18; *gray line*, Gln[116] → His GOB-18.

Asp[120], which is conserved in all MβLs as a Zn2 ligand, was changed to Ser; and Gln[116], distinctive of GOB enzymes, was replaced by a His. The Gln[116] → His mutant, in particular, would be expected to provide a 3-H binding site similar to that found in all B1 and in most B3 MβLs (12, 15, 28, 31).

Gln[116] → His GOB-18 was purified as a mixture of zinc and iron forms, typically with 0.06–0.70 zinc/protein and 0.20–0.60 iron/protein. Remarkably, the total metal content of this mutant never exceeded one equivalent per protein, as determined for wild-type GOB-18. Apo-Gln[116] → His GOB-18 remetallated with Zn(II) bound only one equivalent of Zn(II). The kinetic parameters of zinc-Gln[116] → His GOB-18 showed a partially decreased activity when compared with that of wild-type GOB-18 (Table 1). Addition of 20 μM Zn(II) to the reaction medium gave rise to minor changes in the mutant enzyme activity (data not shown). UV-visible and EXAFS data at the iron edge of holo-Gln[116] → His GOB-18 were identical to those recorded for the wild-type enzyme. Similarly, the paramagnetic ^{1}H NMR spectrum of this mutant showed minor perturbations in the Fe(III) ligand signals when compared with that of the wild-type enzyme (Fig. 4C). The fact that the metal site is largely unperturbed suggests that residue 116 is not a metal ligand neither in wild-type GOB-18 nor in Gln[116] → His GOB-18.

Asp[120] → Ser GOB-18 displayed a markedly decreased metal binding ability for both iron and zinc. The iron binding capacity of Asp[120] → Ser GOB-18 was abolished, and the Zn(II) content reached at most 0.45 Zn(II)/protein (even after exhaustive dialysis against metal containing buffer). Asp[120] → Ser GOB-18 was inactive toward different assayed antibiotics. These data reveal that Asp[120] is a metal ligand, being also essential for catalytic efficiency.

B1 and B2 MβLs have a Cys ligand in the Zn2 site (15, 25). The present three-dimensional model suggests that the only Cys residue present in GOB-18 is far away from the active site. This Cys residue is only accessible to 5,5′-dithiobis-(2-nitrobenzoic acid) under denaturing conditions. To definitively discard the possibility that this Cys residue may serve as a metal ligand in GOB-18, we constructed a Cys[201] → Ser mutant. The metal content, catalytic efficiency, and spectroscopic data of Cys[201] → Ser GOB-18 were similar to those of the wild-type enzyme, indicating the absence of a Cys ligand in the metal binding site, in agreement with the present three-dimensional model and EXAFS data.

DISCUSSION

GOB Enzymes Are Monometallic Lactamases—The biochemical, spectroscopic, and mutagenesis data herein shown allow us to propose that GOB-18 is a mono-metallic MβL, with the catalytic Zn(II) ion bound to Asp[120], His[121], His[263], *i.e.* the canonical Zn2 site (DHH ligand set in subclass B3) (Fig. 5). The coordination sphere would be completed by one or two solvent molecules in the Zn(II) and Fe(III) variants, respectively. The presence of a naturally occurring Gln residue rather than a His at position 116 in GOB-18 resembles the situation found for subclass-B2 MβLs, in which an Asn is found (25, 27). In both cases, the absence of the otherwise conserved His[116] ligand would induce the loss of the Zn1 site. However, engineering a putative 3-H site in GOB-18 does not lead to a dimetallic
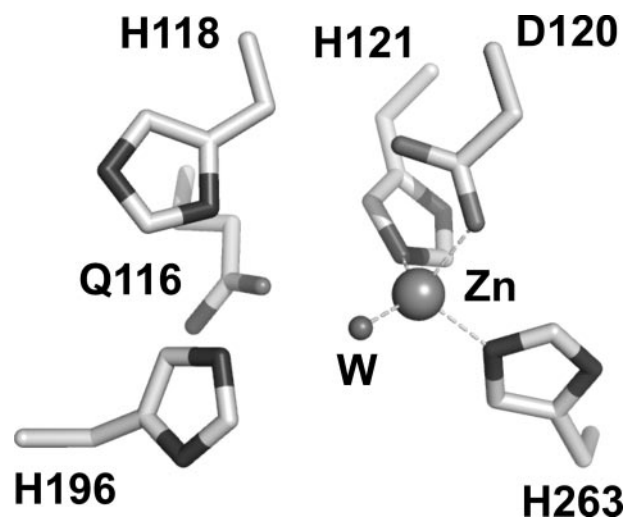

FIGURE 5. **Molecular model of the zinc binding site of GOB-18.** The zinc atom (*Zn*) is shown as a *gray sphere*, and the water molecules (*W*) are shown as *small gray spheres*. Coordination bonds are shown as *dashed lines*.

enzyme, suggesting additional structural differences in the metal site of GOB-18.

GOB enzymes differ by a few point mutations, apparently far from the active site. This allows us to confidently extend our results to all GOB lactamases. GOB MβLs thus present features of B2 (being Zn2-only enzymes) and B3 (based on sequence homology) lactamases. However, two major differences of GOB MβLs with B2 enzymes should be noted: (i) GOB is active even in the presence of 0.1 mM Zn(II), while B2 enzymes are inhibited upon binding of a second Zn(II) equivalent and; (ii) B2 enzymes are selective carbapenemases, while GOB is a broad spectrum MβL. Thus, GOB MβLs are unique in being the only broad spectrum mono-Zn(II) β-lactam hydrolases and in presenting active site mutations within one subclass.

Toward a General Catalytic Mechanism for Metallo-β-Lactamases—The effect of the Zn(II) content on the enzymatic activity in MβLs is still a controversial issue. The Zn1 (3-H) site present in all B1 and in most B3 enzymes, GOB MβLs being the only exception, has been regarded as the catalytic site providing the attacking zinc-bound nucleophile. As inferred from a series of elegant spectroscopic studies, the Zn2 site (DCH ligand set in B1 enzymes and DHH ligands in B3 lactamases) contributes to β-lactam hydrolysis by binding to the bridging β-lactam nitrogen (17, 18, 46). The trapping of hydrolyzed moxalactam in the active site of *S. maltophilia* L1 recently confirmed that both Zn1 and Zn2 are implicated in substrate binding and catalysis in B3 MβLs (47).

The structure of both the free and product-complexed form of the B2 enzyme CphA revealed only one catalytic Zn(II) ion bound to the DCH site (25). This metal ion is also involved in stabilization of the negative charge on the bridging nitrogen atom of the β-lactam ring, as in B1 and B3 enzymes. Thus, the Zn2 site would play the same role in all MβLs, *i.e.* the stabilization of the negative charge developed at the β-lactam nitrogen to favor cleavage of the C–N bond, and the proton delivery through a water molecule bound to it. This is further stressed by the fact that in all studied cases, the rate-determining step is the C–N bond cleavage (that

involves the Zn2 ion) (16, 17, 46, 48). This suggests that a strategy aimed for the design of a general inhibitor could be pursued by targeting the Zn2 site.

The issue that remains unsolved is the identification of the nucleophile in Zn2-only enzymes. The absence of the Zn1 site in B2 lactamases has led to the proposal of a non-metal activated nucleophile, a hypothesis later supported by theoretical and enzymological studies (48, 49). However, the possibility of a Zn2-bound nucleophile cannot been definitively ruled out. The results herein presented reveal that Zn2-only MβLs are not only restricted to B2 subclass and that they can display a broad substrate spectrum. Therefore, a general mechanism of Zn2-only enzymes needs to be definitively elucidated and compared with those of dinuclear and Zn1-only enzymes.

Several reports have indicated that the mono-Zn(II) variants of B1 and B3 enzymes are active (50, 51). Since the first solved MβL structure revealed one metal ion bound to the 3-H site (12), this has been regarded as the catalytic center in monometallic variants. However, spectroscopic data have revealed that when BcII (a well studied B1 lactamases) binds one equivalent of metal ion, it is distributed between the canonical Zn1 and Zn2 sites (52, 53). These data should be reanalyzed at the light of the present evidence, considering that active mono-Zn2 enzymes may also occur among B1 and B3 enzymes other than GOB.

REFERENCES

1. Fisher, J. F., Meroueh, S. O., and Mobashery, S. (2005) *Chem. Rev.* **105,** 395– 424
2. Wilke, M. S., Lovering, A. L., and Strynadka, N. C. (2005) *Curr. Opin. Microbiol.* **8,** 525–533
3. Frere, J. M., Galleni, M., Bush, K., and Dideberg, O. (2005) *J. Antimicrob. Chemother.* **55,** 1051–1053
4. Hall, B. G., Salipante, S. J., and Barlow, M. (2003) *J. Mol. Evol.* **57,** 249 –254
5. Galleni, M., Lamotte-Brasseur, J., Rossolini, G. M., Spencer, J., Dideberg, O., and Frere, J. M. (2001) *Antimicrob. Agents Chemother.* **45,** 660 – 663
6. Garau, G., Di Guilmi, A. M., and Hall, B. G. (2005) *Antimicrob. Agents Chemother.* **49,** 2778 –2784
7. Walsh, T. R., Toleman, M. A., Poirel, L., and Nordmann, P. (2005) *Clin. Microbiol. Rev.* **18,** 306 –325
8. Wang, Z., Fast, W., Valentine, A. M., and Benkovic, S. J. (1999) *Curr. Opin. Chem. Biol.* **3,** 614 – 622
9. Cricco, J. A., Rasia, R. M., Orellano, E. G., Ceccarelli, E. A., and Vila, A. J. (1999) *Coord. Chem. Rev.* **190 –192,** 519 –535
10. Cricco, J. A., and Vila, A. J. (1999) *Curr. Pharm. Des* **5,** 915–927
11. Crowder, M. W., Spencer, J., and Vila, A. J. (2006) *Acc. Chem. Res.* **39,** 721–728
12. Carfi, A., Pares, S., Duee, E., Galleni, M., Duez, C., Frère, J. M., and Dideberg, O. (1995) *EMBO J.* **14,** 4914 – 4921
13. Orellano, E. G., Girardini, J. E., Cricco, J. A., Ceccarelli, E. A., and Vila, A. J. (1998) *Biochemistry* **37,** 10173–10180
14. Fabiane, S. M., Sohi, M. K., Wan, T., Payne, D. J., Bateson, J. H., Mitchell, T., and Sutton, B. J. (1998) *Biochemistry* **37,** 12404 –12411
15. Concha, N., Rasmussen, B. A., Bush, K., and Herzberg, O. (1996) *Structure (Camb.)* **4,** 823– 836
16. Yanchak, M. P., Taylor, R. A., and Crowder, M. W. (2000) *Biochemistry* **39,** 11330 –11339
17. Wang, Z., Fast, W., and Benkovic, S. J. (1999) *Biochemistry* **38,** 10013–10023
18. Wang, Z., Fast, W., and Benkovic, S. J. (1998) *J. Am. Chem. Soc.* **120,** 10788 –10789
19. Garcia-Saez, I., Hopkins, J., Papamicael, C., Franceschini, N., Amicosante, G., Rossolini, G. M., Galleni, M., Frere, J. M., and Dideberg, O. (2003) *J. Biol. Chem.* **278,** 23868 –23873
20. Docquier, J. D., Lamotte-Brasseur, J., Galleni, M., Amicosante, G., Frere, J. M., and Rossolini, G. M. (2003) *J. Antimicrob. Chemother.* **51,** 257–266
21. Materon, I. C., Beharry, Z., Huang, W., Perez, C., and Palzkill, T. (2004) *J. Mol. Biol.* **344,** 653– 663
22. Toney, J. H., Hammond, G. G., Fitzgerald, P. M., Sharma, N., Balkovec, J. M., Rouen, G. P., Olson, S. H., Hammond, M. L., Greenlee, M. L., and Gao, Y. D. (2001) *J. Biol. Chem.* **276,** 31913–31918
23. Toleman, M. A., Simm, A. M., Murphy, T. A., Gales, A. C., Biedenbach, D. J., Jones, R. N., and Walsh, T. R. (2002) *J. Antimicrob. Chemother.* **50,** 673– 679
24. Murphy, T. A., Catto, L. E., Halford, S. E., Hadfield, A. T., Minor, W., Walsh, T. R., and Spencer, J. (2006) *J. Mol. Biol.* **357,** 890 –903
25. Garau, G., Bebrone, C., Anne, C., Galleni, M., Frere, J. M., and Dideberg, O. (2005) *J. Mol. Biol.* **345,** 785–795
26. Hernández Valladares, M., Felici, A., Weber, G., Adolph, H. W., Zeppezauer, M., Rossolini, G. M., Amicosante, G., Frère, J. M., and Galleni, M. (1997) *Biochemistry* **36,** 11534 –11541
27. Crawford, P. A., Yang, K. W., Sharma, N., Bennett, B., and Crowder, M. W. (2005) *Biochemistry* **44,** 5168 –5176
28. Ullah, J. H., Walsh, T. R., Taylor, I. A., Emery, D. C., Verma, C. S., Gamblin, S. J., and Spencer, J. (1998) *J. Mol. Biol.* **284,** 125–136
29. Spencer, J., Clarke, A. R., and Walsh, T. R. (2001) *J. Biol. Chem.* **276,** 33638 –33644
30. Garrity, J. D., Carenbauer, A. L., Herron, L. R., and Crowder, M. W. (2004) *J. Biol. Chem.* **279,** 920 –927
31. Garcia-Saez, I., Mercuri, P. S., Papamicael, C., Kahn, R., Frere, J. M., Galleni, M., Rossolini, G. M., and Dideberg, O. (2003) *J. Mol. Biol.* **325,** 651– 660
32. Bellais, S., Aubert, D., Naas, T., and Nordmann, P. (2000) *Antimicrob. Agents Chemother.* **44,** 1878 –1886
33. Docquier, J. D., Pantanella, F., Giuliani, F., Thaller, M. C., Amicosante, G., Galleni, M., Frere, J. M., Bush, K., and Rossolini, G. M. (2002) *Antimicrob. Agents Chemother.* **46,** 1823–1830
34. Docquier, J. D., Lopizzo, T., Liberatori, S., Prenna, M., Thaller, M. C., Frere, J. M., and Rossolini, G. M. (2004) *Antimicrob. Agents Chemother.* **48,** 4778 – 4783
35. Ausubel, K. M., Brent, R., Kingston, R. E., Moore, R. E., Seidman, I. G., Smith, J. A., and Struhl, K. (1987) *Current Protocols in Molecular Biology*, John Wiley & Sons, New York
36. Costa, G. L., Bauer, J. C., McGowan, B., Angert, M., and Weiner, M. P. (1996) in *In Vitro Mutagenesis Protocols* (Trower, M. K., ed) Humana Press, Totowa, NJ
37. Laemmli, U. K. (1970) *Nature* **227,** 680 – 685
38. Gill, S. C., and von Hippel, P. H. (1989) *Anal. Biochem.* **182,** 319 –326
39. Riener, C. K., Kada, G., and Gruber, H. J. (2002) *Anal. Bioanal. Chem.* **373,** 266 –276
40. Thomas, P. W., Stone, E. M., Costello, A. L., Tierney, D. L., and Fast, W. (2005) *Biochemistry* **44,** 7559 –7569
41. Ankudinov, A. L., Ravel, B., Rehr, J. J., and Conradson, S. D. (1998) *Phys. Rev. B* **58,** 7565–7576
42. McClure, C. P., Rusche, K. M., Peariso, K., Jackman, J. E., Fierke, C. A., and Penner-Hahn, J. E. (2003) *J. Inorg. Biochem.* **94,** 78 – 85
43. Averill, B. A., and Vincent, J. B. (1993) *Methods Enzymol.* **226,** 33–51
44. Marasinghe, G. P., Sander, I. M., Bennett, B., Periyannan, G., Yang, K. W., Makaroff, C. A., and Crowder, M. W. (2005) *J. Biol. Chem.* **280,** 40668 – 40675
45. Que, L., Jr., Lauffer, R. B., Lynch, J. B., Murch, B. P., and Pyrz, J. W. (1987) *J. Am. Chem. Soc.* **109,** 5381–5385
46. McManus-Muñoz, S., and Crowder, M. W. (1999) *Biochemistry* **38,** 1547–1553

47. Spencer, J., Read, J., Sessions, R. B., Howell, S., Blackburn, G. M., and Gamblin, S. J. (2005) *J. Am. Chem. Soc.* **127,** 14439 –14444

48. Sharma, N. P., Hajdin, C., Chandrasekar, S., Bennett, B., Yang, K. W., and Crowder, M. W. (2006) *Biochemistry* **45,** 10729 –10738

49. Xu, D., Xie, D., and Guo, H. (2006) *J. Biol. Chem.* **281,** 8740 – 8747

50. Wommer, S., Rival, S., Heinz, U., Galleni, M., Frere, J. M., Franceschini, N., Amicosante, G., Rasmussen, B., Bauer, R., and Adolph, H. W. (2002) *J. Biol. Chem.* **277,** 24142–24147

51. Costello, A., Periyannan, G., Yang, K. W., Crowder, M. W., and Tierney, D. L. (2006) *J. Biol. Inorg. Chem.* **11,** 351–358

52. de Seny, D., Heinz, U., Wommer, S., Kiefer, M., Meyer-Klaucke, W., Galleni, M., Frere, J. M., Bauer, R., and Adolph, H. W. (2001) *J. Biol. Chem.* **276,** 45065– 45078

53. Hemmingsen, L., Damblon, C., Antony, J., Jensen, M., Adolph, H. W., Wommer, S., Roberts, G. C., and Bauer, R. (2001) *J. Am. Chem. Soc.* **123,** 10329 –10335

The Metallo-β-lactamase GOB Is a Mono-Zn(II) Enzyme with a Novel Active Site

Jorgelina Morán-Barrio, Javier M. González, María Natalia Lisa, Alison L. Costello,
Matteo Dal Peraro, Paolo Carloni, Brian Bennett, David L. Tierney, Adriana S.
Limansky, Alejandro M. Viale and Alejandro J. Vila

Access the most updated version of this article at doi: 10.1074/jbc.M700467200

Alerts:
- When this article is cited
- When a correction for this article is posted

Click here to choose from all of JBC's e-mail alerts

Supplemental material:
http://www.jbc.org/content/suppl/2007/04/03/M700467200.DC1

This article cites 51 references, 17 of which can be accessed free at
http://www.jbc.org/content/282/25/18286.full.html#ref-list-1